energies

MDPI

Article

Hybrid Adaptive Control for PEMFC Gas Pressure

Jing Chen [1], Chenghui Zhang [1], Ke Li [1], Yuedong Zhan [2] and Bo Sun [1,*]

[1] School of Control Science and Engineering, Shandong University, Jingshi-Road 17923, Jinan 250061, China; 201920524@mail.sdu.edu.cn (J.C.); zchui@sdu.edu.cn (C.Z.); like@sdu.edu.cn (K.L.)

[2] Department of Automation, Kunming University of Science and Technology, Jingming-South-Street 727, Kunming 650500, China; ydzhan@kmust.edu.cn

* Correspondence: sunbo@sdu.edu.cn; Tel.: +86-186-0531-8668

Received: 23 August 2020; Accepted: 9 October 2020; Published: 13 October 2020

Abstract: This paper addresses the issues of nonlinearity and coupling between anode pressure and cathode pressure in proton exchange membrane fuel cell (PEMFC) gas supply systems. A fuzzy adaptive PI decoupling control strategy with an improved advanced genetic algorithm (AGA) is proposed. This AGA s utilized to optimize the PI parameters offline, and the fuzzy adaptive algorithm s used to adjust the PI parameters dynamically online to achieve the approximate decoupling control of the PEMFC gas supply system. According to the proposed dynamic model, the PEMFC gas supply system with the fuzzy–AGA–PI decoupling control method was simulated for comparison. The simulation results demonstrate that the proposed control system can reduce the pressure difference more efficiently with the classical control method under different load changes.

Keywords: proton exchange membrane fuel cell; membrane; pressure difference; adaptive control; intelligent optimizing algorithm

1. Introduction

The energy and environment crisis in the 21st century has given impetus to the emergence and development of renewable energy systems [1]. Increasing research and application of renewable energy has become an inevitable global trend. For example, the European Union (EU) set the goal of a low-carbon society in the early 2000s. Data for the EU and for individual EU members show that Germany and France have adopted investment incentives to promote renewable energy, while Denmark and Spain succeeded in structuring their renewable energy sectors [2]. Fuel cells (FC)—as highly efficient and environment-friendly power generating devices that directly convert chemical energy into electric energy—are high-tech devices that can provide a sustainable source of electrical power. The proton exchange membrane fuel cell (PEMFC) is the fifth generation of FCs, and considerable advances achieved in PEMFC technology have made it a promising clean energy technology. PEMFCs not only can complement solar energy, wind energy, and other renewable energy sources, but also have the advantages of low operation temperature and low environmental pollution, flexible use, etc. [3]. PEMFCs are suitable for portable power, hybrid electric vehicles, distributed power stations, and other applications. For example, in 2014, the automobile company Toyota launched Mirai, the first hydrogen fuel cell car, which performed well commercially. Mirai has excellent performance and zero pollution and marks a significant milestone in the technological progress of hydrogen fuel cell vehicles. In summary, PEMFCs have good prospects for commercial development.

Despite these successes, there remain many challenges, such as low safety and reliability, high cost, and short lifetime [4]. For example, the challenges of stability and safety have to be overcome for the popularization and application of PEMFCs. One important reason for these challenges is that the thin proton exchange membrane is subject to tremendous fluctuations in pressure difference

between the anode and cathode due to variations in operating conditions and load changes in automotive applications [5]. Thus, it is necessary to strictly regulate gas pressures to protect the thin proton-exchange membrane and to avoid explosion hazards [6,7]. In the last few years, pressure difference control has been extensively studied. A nonlinear PEMFC gas supply system mathematic model was proposed and validated [8,9]. Based on this model, a control of pressure difference between the cathode and anode was proposed by applying a nonlinear control method based on feedback linearization. Imad et al. [10] proposed a second-order sliding mode multi-input, multi-output control based on a twisting algorithm to regulate the gas pressure on the anode and cathode sides of the PEMFC. Ebadighajari et al. [11] used a model predictive control approach to regulate the pressure difference. Li et al. [12] designed a nonlinear H∞ suboptimal output feedback controller and verified the disturbance rejection ability of the controller. Chen et al. [13] formulated a controller framework related to the common rail theory wherein input disturbances were rejected. An et al. [14] applied a generalized predictive control method to gas supply systems. Their control strategy was validated by comparison with the PID controller. Li et al. [15] studied the effect of pressure differences on the properties of a PEMFC stack and proposed a simple gas pressure control structure based on the PID controller.

However, most of these control methods require complex mathematical operations and are dependent on mathematic models. For better dynamic performance and adaptability to changeable operation conditions and frequent load variation, a model-independent and adaptive control strategy is necessary. This paper proposes a hybrid adaptive control strategy in which the advanced genetic algorithm (AGA) and fuzzy adaptive proportional–integral (PI) algorithm are combined to minimize the pressure differences between the supplied hydrogen and air. Therefore, PEMFC stack systems can be protected under complex operation conditions.

The paper is organized as follows. Section 2 presents the PEMFC gas supply system model and a brief analysis. Section 3 presents the design procedure of the fuzzy–AGA–PI decoupling control in detail. Section 4 describes the evaluation of the performance of the proposed strategy for varied load changes as inputs and compares the strategy with the classical nonlinear control method. Finally, the conclusions are provided in Section 5.

2. PEMFC Gas Supply System Model

The common PEMFC gas supply system structure is shown in Figure 1. Pressurized oxygen (air) is provided to the humidifier for full humidification after regulation by a gas flow controller, and then it is transferred to the cathode channel of the PEMFC to participate in electrochemical reactions. The hydrogen supply route is similar to its oxygen counterpart, except that no compressor is needed for hydrogen given that it comes from a high-pressure hydrogen tank.

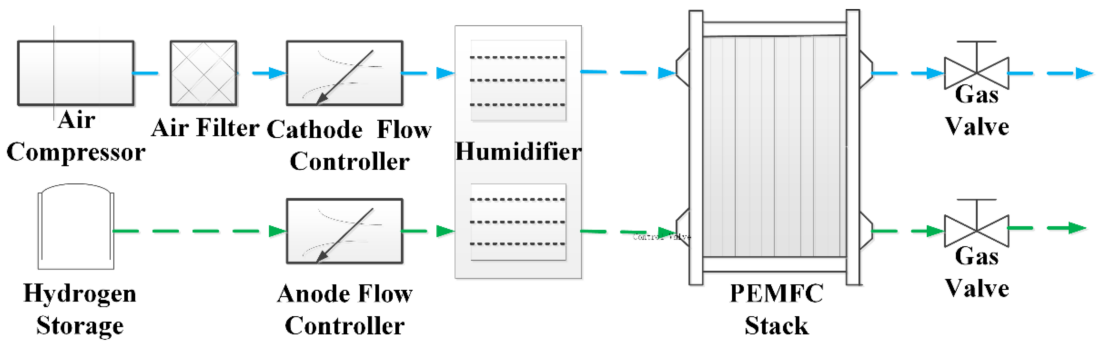

Figure 1. Proton exchange membrane fuel cell (PEMFC) gas supply system structure.

To simplify the dynamic PEMFC model, the following assumptions were made.

1. The gases are ideal.
2. Regarding water management, liquid water stay in the fuel cell and will evaporate to both sides of PEMFC if the humidity become unsaturated [16].
3. The PEMFC stack humidity and temperature are assumed constant because of the slow response time [17].
4. Hydrogen is pure (99.99%), and the air contains a mixture of nitrogen and oxygen in a ratio of 2:8.
5. The Nernst equation is applied.

According to the law of conservation of matter and the ideal gas equation, a PEMFC state equation in the anode can be derived as shown in (1) and (2) [8]:

$$\frac{dp_{H_2}}{dt} = \frac{RT}{V_A}\left[Y_{H_2}K_1H_{2in} - C_1I_{fc} - \left(K_1H_{2in}C_1I_{fc}\right)F_{H_2}\right] \tag{1}$$

$$\frac{dp_{H_2O_a}}{dt} = \frac{RT}{V_A}\left[Y_{H_2}H_{2in}\left(\frac{\varphi_a p_{VS}}{p_{H_2} + p_{H_2Oa} - \varphi_a p_{VS}}\right) - \left(K_1H_{2in} - C_1I_{fc}\right)F_{H_2O_a} - C_2I_{fc}\right] \tag{2}$$

The PEMFC state equations of the cathode are given in (3)–(5):

$$\frac{dp_{O_2}}{dt} = \frac{RT}{V_C}\left[Y_{O_2}K_2O_{2in} - \frac{C_2}{2}I_{fc} - \left(K_2O_{2in} - \frac{C_2}{2}I_{fc}\right)F_{O_2}\right] \tag{3}$$

$$\frac{dp_{N_2}}{dt} = \frac{RT}{V_C}\left[Y_{N_2}K_2O_{2in} - K_2O_{2in}F_{N_2}\right] \tag{4}$$

$$\frac{dp_{H_2O_c}}{dt} = \frac{RT}{V_C}\left[K_2O_{in}\frac{\varphi_c p_{VS}}{p_{O_2} + p_{N_2} + p_{H_2Oc} - \varphi_c p_{VS}} + (C_1 + C_2)I_{fc} - \left(K_2O_{in} + C_1I_{fc} + C_2I_{fc}\right)F_{H_2O_c}\right] \tag{5}$$

Further, the voltage of the PEMFC stack follows (6):

$$V_{stack} = N[E^0 + \frac{RT}{2F}\ln\left(\frac{p_{H_2}\sqrt{p_{O_2}}}{p_{H_2O_c}}\right) - \frac{RT}{2\alpha F}\ln\left(\frac{I_{fc} + I_n}{I_0}\right) - rI_{fc} - m\exp\left(nI_{fc}\right)] \tag{6}$$

where

$$\left.\begin{array}{c} C_1 = NA_{fc}/2F \\ C_2 = 1.2684NA_{fc}/2F \end{array}\right\} \tag{7}$$

$$\left.\begin{array}{c} F_{O_2} = p_{O_2}/\left(p_{O_2} + p_{N_2} + p_{H_2O_c}\right) \\ F_{N_2} = p_{N_2}/\left(p_{O_2} + p_{N_2} + p_{H_2O_c}\right) \\ F_{H_2O_c} = p_{H_2O_c}/\left(p_{O_2} + p_{N_2} + p_{H_2O_c}\right) \\ F_{H_2} = p_{H_2}/\left(p_{H_2} + p_{H_2O_a}\right) \\ F_{H_2O_a} = p_{H_2O_a}/\left(p_{H_2} + p_{H_2O_a}\right) \end{array}\right\} \tag{8}$$

Classically, the water transient flow rate H_2O_c through a membrane is a function of the stack current and humidity. In this study, H_2O_c is the function of current only: H_2Omem = C_1Ifc because we assumed that the humidity is constant with a membrane-average water content.

The nomenclature is provided in Table 1.

Table 1. Nomenclature.

Parameters	Symbols	Units
N	Cell number	/
E^0	Open-circuit voltage in standard pressure	V
R	Gas constant	8.314 J/mol·K
T	Temperature	K
F	Faraday constant	96,485 C mol^{-1}
α	Charges transfer factor	/
I_{fc}	Output current density	A/cm^2
I_0	Exchange current density	A/cm^2
I_n	Internal current density	A/cm^2
m	Mass transfer voltage coefficient	V
n	Mass transfer voltage coefficient	cm^2/A
r	Area-specific resistance	Ω/cm^2
p_{H_2},$p_{H_2O_a}$,p_{O_2},p_{N_2},$p_{H_2O_c}$	Pressures of the hydrogen, oxygen, nitrogen, anode steam, and cathode steam	Pa
F_{O_2},F_{N_2},$F_{H_2O_c}$,F_{H_2},$F_{H_2O_a}$	Pressures fraction of each gas inside the fuel cell	/
$V_{A,}$ V_C	Volume of anode and cathode	cm^3
K_1, K_2	Anode and cathode conversion coefficients, respectively	/
H_{2in}, O_{2in}	Gas flow velocity	mol s^{-1}
φ_a, φ_c	Relative humidity of anode and cathode, respectively	/
p_{vs}	Gas saturation pressure at the 353 K	Pa
Y_{H_2}, Y_{O_2}, Y_{N_2}	The initial mole fractions of hydrogen, oxygen and nitrogen, respectively	/

Based on PEMFC state in Equations (1)–(8), H_2 in and O_2 in are the input variables; P_{H_2} and P_{O_2} are the output variables; and Ifc is the disturbance variable. The MIMO system can be described by Equation (9):

$$\dot{X} = g1(x)u1 + g2(x)u2 + g3(x)d \tag{9}$$

where

$$X = \begin{bmatrix} p_{H_2} \\ p_{H_2O_a} \\ p_{O_2} \\ p_{N_2} \\ p_{H_2O_c} \end{bmatrix};\ U = \begin{bmatrix} H_{2in} \\ O_{2in} \end{bmatrix};\ d = I_{fc}$$

$$g1(x) = \begin{bmatrix} \frac{RT}{V_A}K_1\left(Y_{H_2} - F_{H_2}\right) \\ \frac{RT}{V_A}\left(\frac{\varphi_a p_{VS}}{p_{H_2} + p_{H_2Oa} - \varphi_a p_{VS}} - K_1 F_{H_2O_a}\right) \\ 0 \\ 0 \\ 0 \end{bmatrix}$$

$$g2(x) = \begin{bmatrix} 0 \\ 0 \\ \frac{RT}{V_C}K_2\left(Y_{O_2} - F_{O_2}\right) \\ \frac{RT}{V_C}K_2\left(Y_{H_2} - F_{N_2}\right) \\ \frac{RT}{V_C}K_2\left(\frac{\varphi_c p_{VS}}{p_{O_2} + p_{N_2} + p_{H_2Oc} - \varphi_c p_{VS}} - F_{H_2O_c}\right) \end{bmatrix}$$

$$g2(x) = \begin{bmatrix} -\frac{RT}{V_A}C_1(1 + F_{H_2}) \\ \frac{RT}{V_A}\left(C_1 F_{H_2O_a} - C_2\right) \\ -\frac{RT}{2V_C}C_2(1 - F_{O_2}) \\ 0 \\ \frac{RT}{V_C}(C_1 + C_2)\left(1 - F_{H_2O_c}\right) \end{bmatrix}$$

In the presented model, which is based on Equations (1)–(8), the gas systems of the anode and cathode are coupled to obtain a complex system. In a PEMFC power generation system, the pressure and flow of the reaction gas in the PEMFC change with changes in the load [9]. To prevent damage to the membrane, the pressure difference should be minimized [18]. In addition, the performance of the PEMFC is a function of the gas pressure, which has a non-negligible influence on the FC performance [19]. Hence, it is desirable to adjust the partial pressures at the cathode and anode to stabilize at the set value, via an effective method, such as the decoupling control method, to avoid unwanted pressure fluctuation and reduce the pressure difference between the anode and the cathode when the PEMFC stack experiences large and frequent changes in the load.

3. Fuzzy–AGA–PI Decoupling Control Design

To achieve better decoupling control, an indirect decoupling algorithm was adopted, and the fuzzy subspace was decomposed based on the multivariable fuzzy rules. The fuzzy control algorithm is enforceable in a time-varying system or a pure hysteresis nonlinear system [20], including the complex PEMFC model, because it does not depend on the control object model. By combining the fuzzy adaptive algorithm with the AGA–PI control algorithm as done in the proposed feed-forward decoupling control system, the hydrogen gas pressure loop and oxygen gas pressure loop can be controlled to achieve the dynamic decoupling compensation of PI control parameters so that the coupled loops can be treated as two equivalent single loops. The hybrid adaptive fuzzy–AGA–PI decoupling control system of the PEMFC gas supply system is shown in Figure 2.

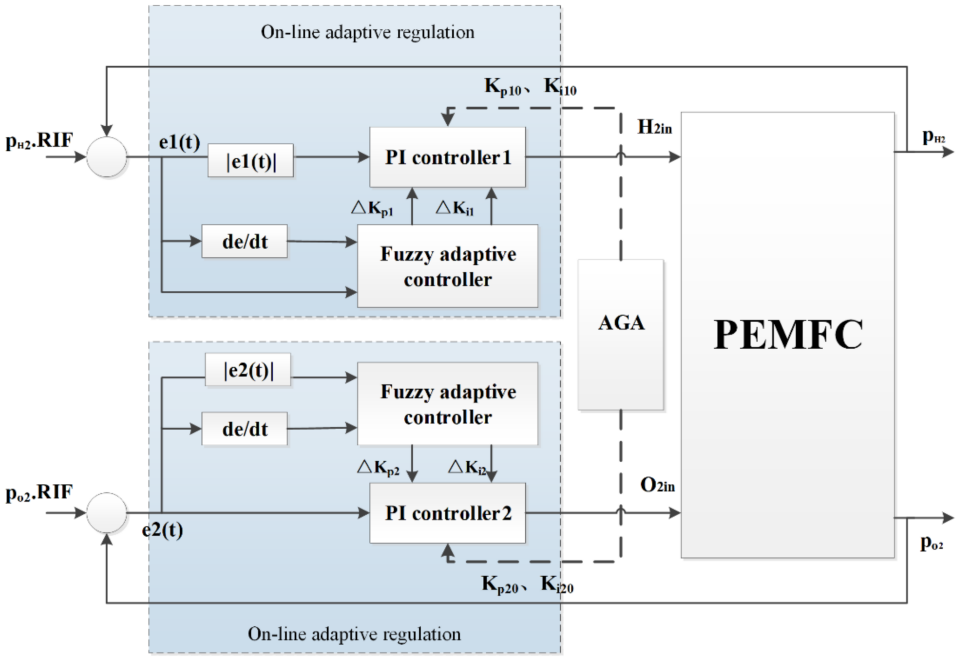

Figure 2. Hybrid adaptive fuzzy–AGA–PI decoupling control system.

First, the parameters of the PI controller were optimized by AGA. Then, the error e and the change in the error, ec, were the input variables for the fuzzy controller [19]. The fuzzy controller was run online to adaptively adjust K_{p0} and K_{p1} of the AGA–PI controller by outputs ΔK_p and ΔK_i, which obey the designed fuzzy rules.

3.1. AGA–PI Control Algorithm Design

First, an AGA was utilized to optimize the parameters of the PI controller offline and to improve the control performance of the pressure difference between p_{H_2} and p_{O_2}.

The traditional PID controller is still widely used in industrial process control because of its simple structure, strong handling ability, and great robustness. The PID controller has three parameters, *Kp*, *Ki*, and *Kd*. *Kd* is the differential of error with time, and it has a function of advanced control. *Kd* is not suitable for the PEMFC gas supply system because the pre-control will result in the abrupt change of pressure with changes in the load. Hence, PI control was chosen instead of PID control in this study.

The genetic algorithm (GA), which is a stochastic global search method based on the principle of natural selection and evolution, is frequently used in many engineering applications to find solutions to optimization problems. The heuristic search of GAs is based on the principle of survival of the fittest [21]. GAs start the optimization process with an initial random population. The objective function is the function responsible for assigning the fitness value to each member of the population. Individuals that represent better solutions are awarded higher fitness values, and thus, they survive for more generations. The successive generations of the population are created by the genetic operators reproduction, crossover, and mutation to yield better solutions to achieve the optimal solution to the problem. The above steps are repeated until the predetermined criteria are met. However, the traditional GA is likely to fall into local optimum solutions and cannot obtain globally optimal solutions [22]. In this study, the basic GA was improved to avoid the local optimum, and a simulated annealing algorithm was added to execute the local searching operation to obtain the advanced genetic algorithm (AGA) [23]. A flow chart of the proposed AGA control is shown in Figure 3.

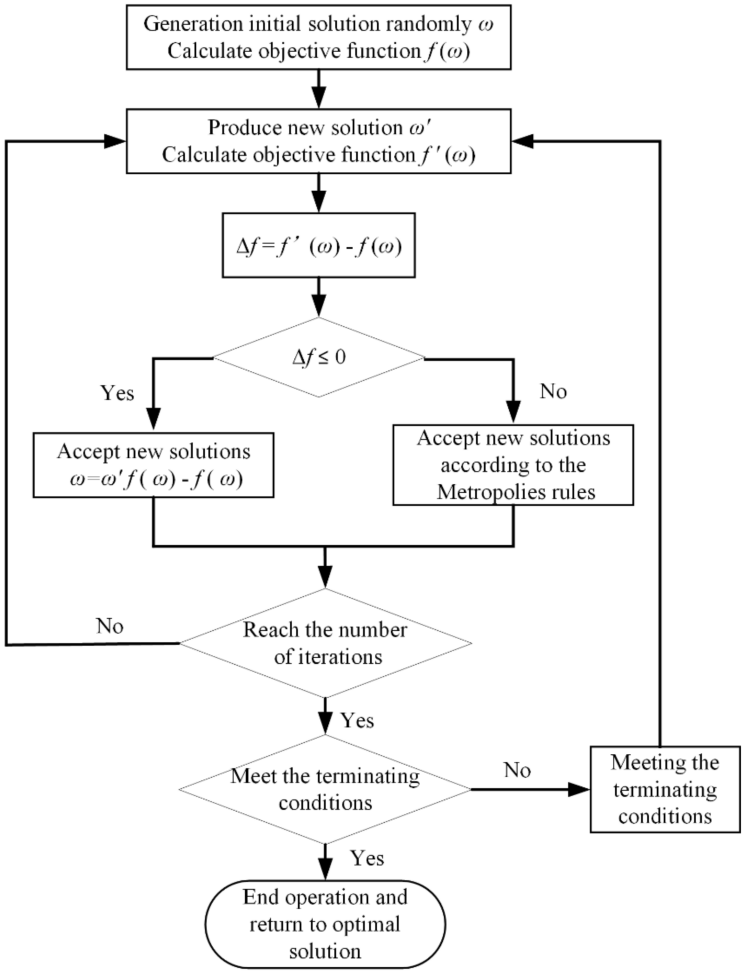

Figure 3. Flow chart of the advanced genetic algorithm (AGA).

The main parameters defined in AGA control include the population size *M*, iteration number *G*, crossover probability *Pc*, and mutation probability *Pm* [24]. There is no theoretical definition

for selecting the aforementioned parameters, although the empirical range of parameter settings has been reported by some researchers. Floudas et al. [25] studied the influence of parameters on the performance of GA systematically and proposed a set of widely applied standard parameters. Laoufi et al. [26] discussed the definition of parameters in detail and presented a general range of *M*, *G*, *Pm*, and *Pc*. The parameters chosen in this study were based on the cited publications and were combined with the simulation results. Thus, the following values were obtained:

$$\left.\begin{array}{c} M = 200 \\ G = 100 \\ P_c = 0.5 \\ P_m = 0.005 \end{array}\right\} \tag{10}$$

For realizing a better system dynamic response, the integral of time and squared errors (ITSE) should be minimized, i.e., the objective function is as shown in Equations (11):

$$f = \min(ITSE) = \int_0^{+\infty} te^2(t)dt \tag{11}$$

where *t* is running time of the system and *e(t)* is the deviation between the input and the step response of a unit function response of the system.

According to the presented optimization strategy and parameters settings, the AGA was programmed to optimize the parameters of the PI controller. After 100 generations of evolutionary search, the AGA converged, and the optimization result was obtained based on the model indicated by Equations (1)–(8). The results are as follows:

$$\begin{array}{c} K_{p10} = 346.1 \\ K_{i10} = 598.2 \\ K_{p20} = 486.7 \\ K_{i20} = 398.9 \end{array}$$

3.2. Fuzzy–AGA–PI Decoupling Control Design

The hybrid adaptive fuzzy–AGA–PI decoupling control is an improvement on the AGA–PI controller. It can realize adaptive control by adjusting the optimized PI parameters online with multifarious loading changes. The design process of the fuzzy controller involves three main steps: fuzzification, fuzzy inference, and defuzzification [27].

As shown in Figure 2, the input values of the fuzzy controller are *e* and *ec*, and the output values are ΔK_p and ΔK_i (see Equations (12)–(14)):

$$e = \left| p_x - p_x^{ref} \right| \tag{12}$$

$$ec = de/dt \tag{13}$$

$$\left.\begin{array}{c} K_p = K_{p0} + \Delta K_p \\ K_i = K_{i0} + \Delta K_i \end{array}\right\} \tag{14}$$

where *e* is the absolute value of the difference between p_x and p_x^{ref}; *x* is H_2 or O_2; *ec* is the variation rate of *e*; K_{p0} and K_{i0} are the initial values of the parameters; and K_p and K_i are the parameters of AGA optimized PI controller changed by the fuzzy adaptive algorithm.

The adapted triangular membership function can be described as shown in Equations (15) [28]:

$$\mu(x) = \left\{ \begin{array}{l} \frac{x-a}{b-a}, x \in (a, b) \\ \frac{x-c}{b-c}, x \in (b, c) \end{array}\right. \tag{15}$$

where a, b, and c are the constants of the fuzzy domain.

The ranges of inputs and outputs are defined according to the simulation outputs of the AGA–PI control system and experiments. These ranges are listed in Tables 2 and 3.

Table 2. Ranges of the input and out variables for H_2.

Variable	$e1$	$ec1$	ΔK_{p1}	ΔK_{i1}
Range	[0—0.006]	[−3—3]	[−250—250]	[−200—200]

Table 3. Ranges of the input and out variables for O_2.

Variable	$e2$	$ec2$	ΔK_{p2}	ΔK_{i2}
Range	[0—0.018]	[−3—3]	[−260—260]	[−220—220]

The rule tables are provided in Tables 4 and 5. Seven membership functions are used for the inputs and outputs: negative big (NB), negative middle (NM), negative small (NS), zero (Z0), positive small (PS), positive middle (PM), and positive big (PB). The fuzzy rules are designed in accordance with the given PEMFC gas supply system, e.g., the surface values listed in Table 4 for the anode are shown in Figure 4. For the same control effect, the algorithm complexity of time and space are reduced by removing the fuzzy inferences on the negative part of e according to (12).

Table 4. Fuzzy rules for proportional gain ΔK_p in the fuzzy control algorithm.

ΔK_i		ec						
		NB	NM	NS	ZO	PS	PM	PB
e	ZO	ZO	ZO	PS	PS	PS	PM	PM
	PS	ZO	ZO	PS	PS	PM	PM	PB
	PM	ZO	PS	PS	PM	PM	PB	PB
	PB	PS	PS	PM	PM	PB	PB	PB

Table 5. Fuzzy rules for integral gain ΔK_i in the fuzzy control algorithm.

ΔK_i		ec						
		NB	NM	NS	ZO	PS	PM	PB
e	ZO	NM	NM	NS	ZO	PS	PM	PM
	PS	NM	NS	ZO	PS	PS	PM	PB
	PM	ZO	ZO	PS	PS	PM	PB	PB
	PB	ZO	ZO	PS	PM	PM	PB	PB

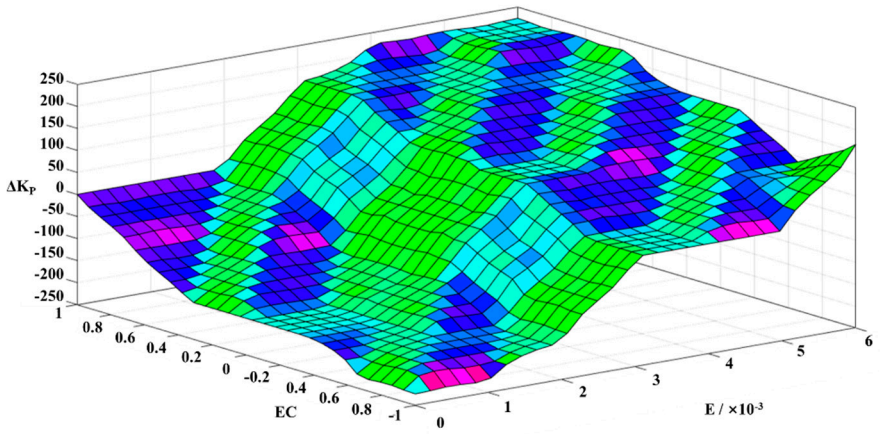

Figure 4. Surface of fuzzy rules for proportional gain ΔK_p for the anode.

The weighted averages method can be described as shown in (16):

$$Z_0 = \frac{\sum_{i=1}^{n} Z_i \mu_c(Z_i)}{\sum_{i=1}^{n} \mu_c(Z_i)} \tag{16}$$

where Z_0 is the numerical value, Z_i is the membership value, and $\mu_c(Z_i)$ is the fuzzy variable.

4. Simulation Results

The proposed hybrid adaptive fuzzy–PI decoupling control was tested by using MATLAB/Simulink. For simplicity, the fuel processor, water and heat management, and air compressor models were not considered in the simulation.

The aim of the controller is to minimize the pressure difference between the anode and cathode by maintaining the pressure at the set point. Because of the assumption that oxygen accounts for one-fifth of the air, the setpoint gas pressure of hydrogen and oxygen were maintained at 3 and 0.6 atm, respectively (1 atm = 0.1 MPa), under irregular load variations; thus, the pressure difference between the cathode and anode was minimized [8]. Experimental data reported by Hamelin et al. [29] were used for validating the presented dynamic PEMFC model. The nominal values of the simulation parameters are listed in Table 6.

Table 6. PEMFC simulation parameters.

Parameters	N	E^0	R	F	α	Afc	V_A	Vc
Values	35 /	1.032 (V)	8.314 (J/mol·K)	96,485 (C/mol)	0.5 /	232 (cm^2)	5 (cm^3)	10 (cm^3)
Parameters	T	m	n	r	Pvs	ka	kc	
Values	353 (K)	2.11×10^{-5} (V)	8×10^{-3} (cm^2/mA)	0.245 (Ω/cm^2)	32 (KPa)	7.034×10^{-4} (mol/s)	7.036×10^{-4} (mol/s)	

The response curves of the pressure in the anode and cathode corresponding to the load changes shown in Figure 5 are shown in Figures 6 and 7, respectively, corresponding to the fuzzy–AGA–PI control system and classical nonlinear control system. It is noteworthy that the output voltage improvement is not evident in Figure 6, due to the logarithm function between voltage and gas pressure, small pre factor (RT/2F), and fast response time. However, other simulation results in Figure 7a,b show that the proposed control strategy has a significantly better transient response than the classical nonlinear control; hence, the proposed strategy can maintain the gas pressure at an ideal value more efficiently as a whole.

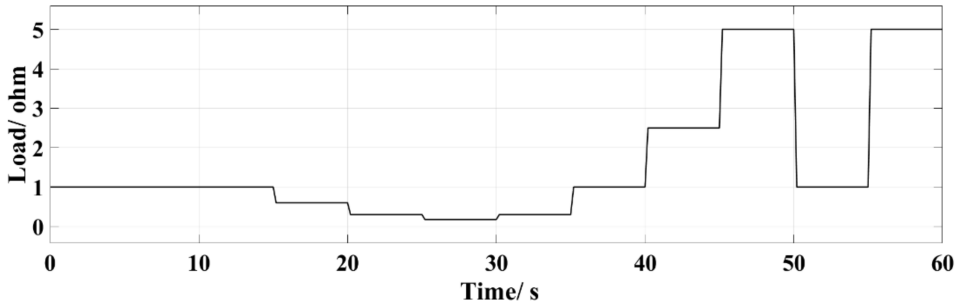

Figure 5. Load variation profile.

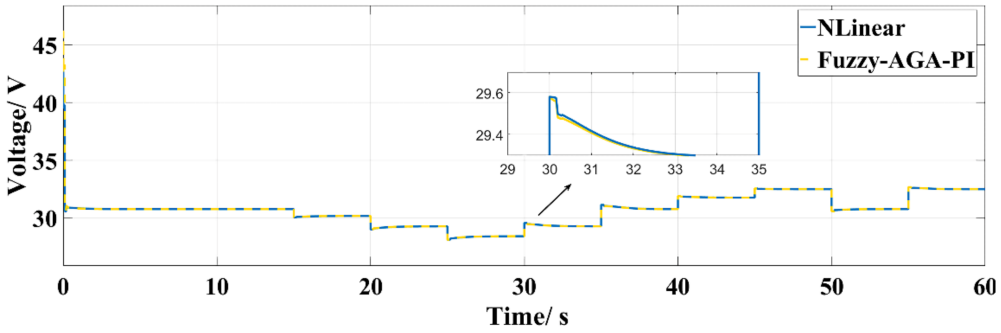

Figure 6. Voltage curve during load variation.

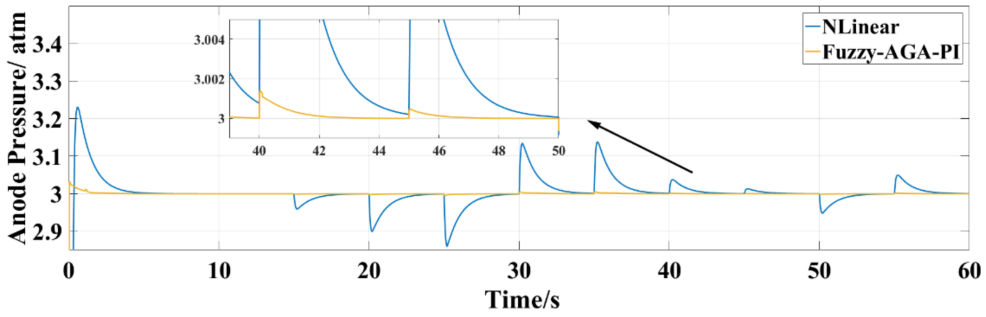

(**a**)

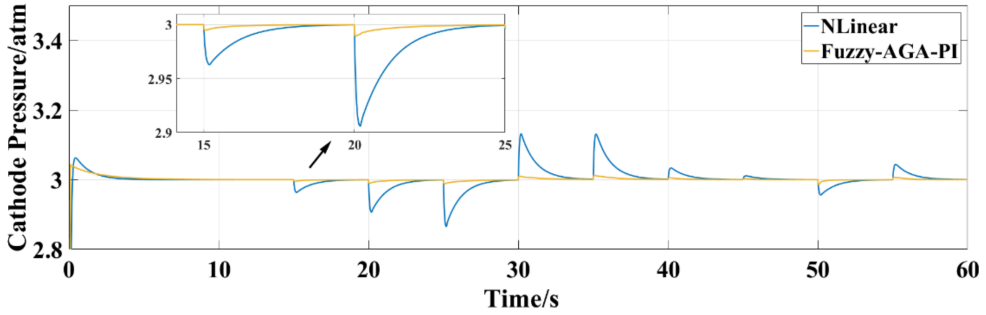

(**b**)

Figure 7. Performance curve of anode and cathode pressures during load variation.

Furthermore, five representative moments of changes in the load were selected for a detailed analysis. They are the start, the moments when the load decreases or increases slightly, and the moments when the load decreases or increases considerably. The moments are shown in Figures 8–10.

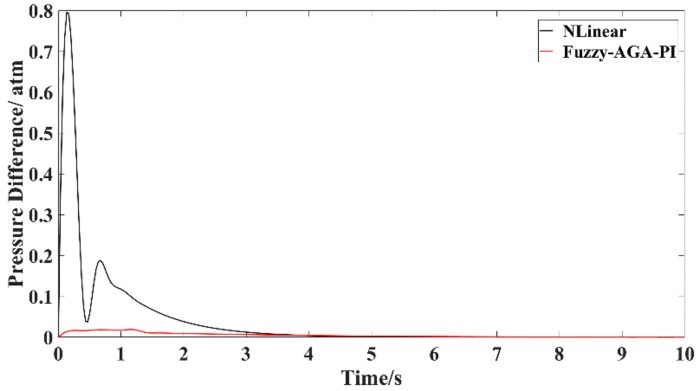

Figure 8. Variations in pressure difference when the PEMFC operation is started.

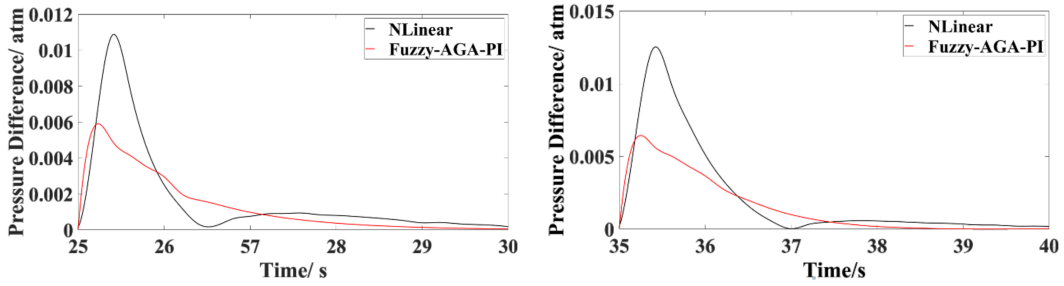

Figure 9. Two load changing moments with slight changes in the load.

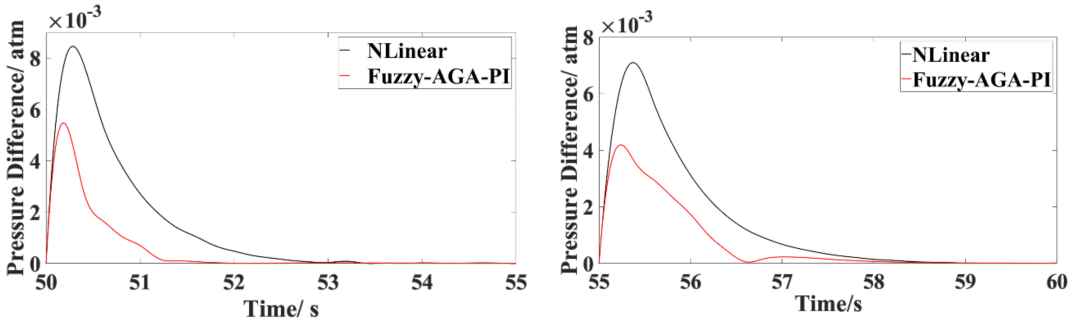

Figure 10. Two moments of large changes in the load.

As shown in Figure 8, the fuzzy–AGA–PI adaptive control performs considerably better in terms of the wave stability of gas pressure in the gas supply system of the PEMFC when the PEMFC operation is started. The pressure difference is as high as 0.78 atm, which poses a safety risk for the proton exchange membrane [30]. However, the proposed control strategy reduces the gas pressure to less than 0.016 atm because of its adaptability and approximate decoupling.

Figure 9 shows the responses of gas pressure difference when the load changes slightly. The fuzzy–AGA–PI control can reduce the overshoot to 45% and 50% compared to nonlinear control but needs a longer adjusting time. However, the fuzzy–AGA–PI control system can provide better protection against high pressure differences than possible with the nonlinear control system from the viewpoint of the application.

The fuzzy–AGA–PI control is still valid even under large changes in the load, e.g., increase and decrease by 4 Ω, as shown in Figure 9. The proposed control decreases the overshoot to 30% and 42% relative to the nonlinear control under two operation conditions and requires a shorter convergence time.

In conclusion, the simulation results show that the hybrid adaptive PI control system has better response characteristics than the classical nonlinear control regardless of small or large changes in the load, especially at the time of starting of the PEMFC operation. Therefore, the fuzzy–AGA–PI control can reduce the pressure difference between the cathode and anode in runtime PEMFCs more efficiently.

5. Conclusions

A hybrid adaptive PI decoupling control—more specifically, a fuzzy adaptive PI decoupling control based on optimization by the AGA—is proposed to achieve the nonlinear and approximate decoupling control of a PEMFC gas supply system. Comparison of the simulation results obtained using the proposed and the classical nonlinear control methods shows that the proposed control strategy not only can deliver smooth static tracking for setting the pressure, but also can improve the dynamic performance under various load changes. According to the requirements of practical PEMFC applications, the proposed control strategy can improve the FC performance and protect the proton membrane from damage caused by pressure differences. Because of its excellent control effect and wide adaptability, the presented hybrid adaptive PI decoupling control strategy can also be applied to

the other components of PEMFC systems, including the control of water and heat management, air compressor, and fuel processor.

Author Contributions: J.C. proposed the idea, performed the experiments, and wrote the paper; C.Z. analyzed the data; K.L. conceived and designed the experiments; Y.Z. revised the paper; and B.S. supervised the overall work and the overall structure of the paper. All authors have read and agreed to the published version of the manuscript.

Funding: This research was funded by the National Natural Science Foundation of China (grant numbers 61821004, 61733010), Department of Science and Technology of Shandong Province (grant number 2019JZZY010901), Natural Science Foundation of Shandong province (grant number ZR2019ZD09), Innovation Team Project of Jinan Science and Technology Bureau (grant number 2019GXRC003) and the Young Scholars Program of Shandong University (grant number 2016WLJH29).

Conflicts of Interest: The authors declare no conflict of interest.

References

1. Brodny, J.; Tutak, M. Analyzing similarities between the european union countries in terms of the structure and volume of energy production from renewable energy sources. *Energies* **2020**, *13*, 913. [CrossRef]
2. Fang, K.; Zhou, Y.; Wang, S.; Ye, R.; Guo, S. Assessing national renewable energy competitiveness of the G20: A revised Porter's Diamond Mode. *Renew. Sustain. Energy Rev.* **2018**, *93*, 719–731. [CrossRef]
3. Lee, C.Y.; Chen, C.H.; Tsai, C.H. Development of an internal real-time wireless diagnostic tool for a proton exchange membrane fuel cell. *Sensors* **2018**, *18*, 213. [CrossRef] [PubMed]
4. Liu, H.; Chen, J.; Hissel, D.; Su, H.Y. Short-term prognostics of PEM fuel cells: A comparative and improvement study. *IEEE Trans. Ind. Electron.* **2019**, *66*, 6077–6086. [CrossRef]
5. Roy, S.; Ragunath, S. Emerging membrane technologies for water and energy sustainability: Future prospects, constraints and challenges. *Energies* **2018**, *11*, 2997. [CrossRef]
6. Chen, Y.; Wang, N. Cuckoo search algorithm with explosion operator for modeling proton exchange membrane fuel cells. *Int. J. Hydrogen Energy* **2019**, *44*, 3075–3087. [CrossRef]
7. Chen, B.; Cai, Y.; Shen, J.; Tu, Z.; Chan, S.H. Performance degradation of a proton exchange membrane fuel cell with dead-ended cathode and anode. *Appl. Therm. Eng.* **2018**, *132*, 80–86. [CrossRef]
8. Na, W.K.; Gou, B.; Diong, B. Nonlinear control of PEM fuel cells by exact linearization. *IEEE Trans. Ind. Appl.* **2007**, *43*, 1426–1433. [CrossRef]
9. Na, W.; Gou, B.; Kim, J.H. Complementary cooperation dynamic characteristics analysis and modeling based on multiple-input multiple-output methodology combined with nonlinear control strategy for a polymer electrolyte membrane fuel cell. *Renew. Energy* **2020**, *149*, 273–286. [CrossRef]
10. Matraji, I.; Laghrouche, S.; Wack, M. Pressure control in a PEM fuel cell via second order sliding mode. *Int. J. Hydrogen Energy* **2012**, *37*, 16104. [CrossRef]
11. Ebadighajari, A.; Devaal, J.; Golnaraghi, F. Multivariable control of hydrogen concentration and fuel over-pressure in a polymer electrolyte membrane fuel cell with anode re-circulation. In Proceedings of the 2016 American Control Conference (ACC), Boston, MA, USA, 6–8 July 2016; pp. 4428–4433.
12. Li, Q.; Chen, W.R.; Liu, S.K.; Cheng, Z.L.; Liu, X.Q. Application of multivariable H∞ suboptimal control for proton exchange membrane fuel cell pressure control system. *Proc. CSEE* **2010**, *30*, 123.
13. Chen, F.X.; Yu, Y.; Li, Y.; Chen, H.C. Control system design for proton exchange membrane fuel cell based on a common rail (II): Optimization and schedule scheme for the common rail. *Int. J. Hydrogen Energy* **2017**, *42*, 4294–4301. [CrossRef]
14. An, A.M.; Zhang, H.C.; Liu, X.; Chen, L.W. Generalized predictive control for gas supply system in a proton exchange membrane fuel cell. *Adv. Mater. Res.* **2012**, *512*, 1380–1388. [CrossRef]
15. Li, Y.; Zhao, X.; Tao, S.; Li, Q.; Chen, W. Experimental study on anode and cathode pressure difference control and effects in a proton exchange membrane fuel cell system. *Energy Technol.* **2015**, *3*, 946–954. [CrossRef]
16. Purkrushpan, J.T.; Stefanopoulou, A.G.; Peng, H. Control of fuel cell breathing. *IEEE Control Syst. Mag.* **2004**, *24*, 30–46.
17. Qu, K.; Yuan, W.W.; Choi, M.; Yang, S.; Kim, Y.B. Performance increase for an open-cathode PEM fuel cell with humidity and temperature control. *Int. J. Hydrogen Energy.* **2017**, *42*, 29850–29862.
18. Selvaray, A.S.; Rajagopal, T.K.R. Numerical investigation on the effect of flow field and landing to channel ratio on the performance of PEMFC. *Int. J. Energy Res.* **2020**, *44*, 171–191. [CrossRef]

19. Chen, J.; Zhan, Y.D.; Guo, Y.G.; Zhu, J.G.; Li, L.; Liang, B. Fuzzy adaptive PI decoupling control for gas supply system of proton exchange membrane fuel cell. In Proceedings of the 2018 21st International Conference on Electrical Machines and Systems (ICEMS), Jeju, Korea, 7–10 October 2018.
20. Li, D.; Liu, L.; Liu, Y.J.; Tong, S.C.; Chen, P.C.L. Fuzzy Approximation-Based Adaptive Control of Nonlinear Uncertain State Constrained Systems with Time-Varying Delays. *IEEE Trans. Fuzzy Syst.* **2020**, *28*, 1620–1630. [CrossRef]
21. Arunasalam, P.; Seetharamu, K.N.; Azid, I.A. Determination of thermal compact model via evolutionary genetic optimization method. *IEEE Trans. Compon. Packag. Technol.* **2005**, *28*, 345–352. [CrossRef]
22. Wu, K.H.; Wang, J.; Yang, B.; Feng, L.; Zhang, X.L.; Chen, L. Optimal strategy of reactive in distribution network based on GA enhanced Trust-Tech technology. *J. Eng.* **2017**, *13*, 1242.
23. Abdelouahhab, J.; Abdellah, E.B.; Ahmed, E.K. Multipass Turning Operation Process Optimization Using Hybrid Genetic Simulated Annealing Algorithm. *Model. Simul. Eng.* **2017**, *2017*, 1–10.
24. Huang, C.L.; Wang, C.J. A GA-based feature selection and parameters optimization for support vector machines. *Expert Syst. Appl.* **2006**, *31*, 231–240. [CrossRef]
25. Floudas, C.A.; Pardalos, P.M. Quadratic Programming Test Problems. In *A Collection of Test. Problems for Constrained Global Optimization Algorithms*; Springer: Berlin/Heidelberg, Germany, 1990; pp. 6–20.
26. Laoufi, A.; Hazzab, A.; Rahli, M. Economic power dispatch using fuzzy-genetic algorithm. *Int. J. Appl. Eng. Res.* **2008**, *3*, 973–4562.
27. Mohammed, A.; Bayford, R.; Demosthenous, A. A framework for adapting deep brain stimulation using Parkinsonian state estimates. *Front. Neurosci.* **2020**, *14*, 17. [CrossRef]
28. Lee, C.C. fuzzy logic in control systems: Fuzzy logic controller—Part I. *IEEE Trans. Syst. Man Cybern.* **1990**, *20*, 404. [CrossRef]
29. Hamelin, J.; Abbossou, K.; Laperroere, A.; Laurencelle, F.; Bose, T.K. Dynamic behavior of a PEM fuel cell stack for stationary applications. *Int. J. Hydrogen Energy* **2001**, *26*, 625–629. [CrossRef]
30. Pukrushpan, J.T.; Stefanopoulou, A.G.; Peng, H. *Control of Fuel Cell Power Systems: Principles, Modeling and Analysis and Feedback Design*; Springrr: Berlin/Heidelberg, Germany, 2004.